THE PUBLISHING HOUSE
OF THE ROMANIAN ACADEMY

PROCEEDINGS OF THE ROMANIAN ACADEMY, Series A,
Volume 18, Number 2/2017, pp. 150–157

EXPERIMENTAL PROGRAM FOR IMPACT TESTS ON A HONEYCOMB CORE COMPOSITE MATERIAL

Horia Alexandru PETRESCU, Anton HADĂR, Ştefan Dan PASTRAMĂ

"Politehnica" University of Bucharest, Department of Strength of Materials,
Splaiul Independenței nr. 313, Sector 6, 060042, Bucharest, Romania.
Corresponding author: Ştefan Dan PASTRAMĂ, E-mail: stefan.pastrama@upb.ro

Abstract. In this paper, an experimental program of impact tests for a honeycomb core composite material with skins made of epoxy resin reinforced with glass fiber is presented. Several configurations, involving two different core heights and two or three layered skins were investigated in order to find the best one in terms of impact energy absorption. Several criteria were used to evaluate the behavior of specimens subjected to low velocity impact: damage of the core following the impact, behavior of core at impact, possible penetration of the skin, variation of impact force in time during impact and type of force drop, and, finally, the average impact force, defined as the total absorbed strain energy divided by the tup displacement. Conclusions were drawn following the recording of the variation of the impact force and strain energy of the specimens in drop-weight tests with different impact speeds. Finally, a numerical study using the finite element method was undertaken in order to understand the impact process and to verify the correctness of the experimental results. For this, one of the studied specimens was modeled and impact was simulated in the same conditions as the ones used in the experimental program. The variation of the impact force in time was obtained numerically and compared with the experimental data, showing a good agreement.

Key words: sandwich structure, honeycomb core, impact, strain energy, finite element.

1. INTRODUCTION

Honeycomb structures are made of arrays of hollow hexagonal cells separated by thin vertical walls. In practice, they are manufactured using different materials (paper, thermoplastics, aluminum, fiber reinforced plastics, etc.). Common use of such structures can be found in aerospace or automotive industry, furniture, packaging, logistics, etc. A stratified honeycomb core material (Fig. 1) is a class of composite materials manufactured of two thin skins attached to a lightweight and thick core. The core material is normally a low strength material, but its higher thickness provides the sandwich composite with high bending stiffness with overall low density.

Honeycomb cores are available in a variety of materials for sandwich structures. These range from paper or cardboard for applications where low strength, stiffness or loads appear (such as home doors) to aluminum for high strength and stiffness, extremely lightweight components for aircraft structures [1]. Laminates of glass or carbon fiber reinforced thermoplastics or mainly thermoset polymers (unsaturated polyesters, epoxies) are widely used as skin materials.

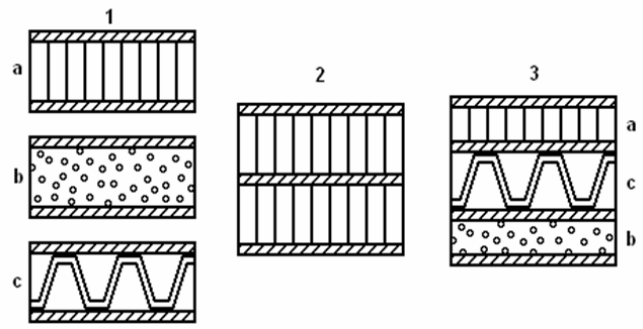

Fig. 1 – Sandwich structured composite with simple core (1), double core (2), triple hybrid core (3); a – honeycomb structure, b – rigid foam, c – aluminum sheets.

Dynamic tests on honeycomb core structures are often performed using drop-weight impact devices in order to assess the energy absorption profile of such materials.

Several researchers have drawn their attention to the impact testing of composite materials with honeycomb cores. A study of the lateral compressive

response of hexagonal honeycomb panels from the initial elastic regime to a fully crushed state was presented by Wilbert *et al*. [2]. The authors tested expanded hexagonal, double walled honeycomb panels made of aluminum alloy, which were laterally compressed quasi statically between rigid platens under displacement control. Conclusions were drawn regarding the collapse stress and crushing stress of the panels. The crushing phenomenon of specimens made of Nomex aluminum alloy and paper under compression was studied in [3]. Here, the authors modeled low velocity/low energy impact showing that honeycomb core subjected to compression can be modeled by a grid of nonlinear springs. The same core structure with carbon epoxy skins having different number of plies was investigated for the low-velocity impact response by Meo *et al*. [4] in order to investigate damage initiation, damage propagation, and failure mechanisms. Similar experimental tests were presented by Yamashita and Gotoh [5]. Here, the experimental determinations are accompanied by numerical simulations in order to find the effect of the cell shape and the foil thickness on crush behavior. A finite element methodology has been developed by Chawla *et al*. [6] for predicting the behavior of honeycomb structures. Dynamic analysis of hexagonal aluminum honeycomb structures was carried out by the authors using a commercial finite element code, and the result are verified against experimental data. A relationship between the crushing behavior of honeycomb and simulation parameters was proposed. Griškevičius *et al*. [7] performed experimental investigation of deformation behavior of sandwich structures with honeycomb core in the cases of quasi-static and dynamic loading. Also, numerical modelling by finite element method of sandwich structures behavior under impact loading was presented by the authors. The investigated structures were sandwich composites made from woven glass fiber and polyvinyl-ester resin composite face sheets and polypropylene hexagonal honeycomb. Impact behavior and energy absorption of honeycomb structures with paper core and paper skin was presented by Wang [8] in order to show a methodology to optimize the design of such material. The failure response of honeycomb aluminum sandwich panels subjected to low-velocity impact is discussed in [9]. The authors propose also three-dimensional finite element analyses of a honeycomb sandwich plate and a rigid impactor, enabling further understanding of the parameters affecting the initiation and propagation of impact damage. Dear *et al*. [10] presented drop-weight tests on specimens prepared from sheet molding compound, glass mat thermoplastic and honeycomb sandwich panels employing different skin and core materials. The authors studied the variation of different parameters during impact in order to compare the behavior of different materials from this point of view. Low velocity impact of honeycomb core composite materials is also investigated both experimentally and with numerical methods by other authors [11–16]. A comprehensive review of the past and current research progress on dynamic response of composites sandwich structures, including honeycomb sandwich structures, subjected to low-velocity impact was published by Chai and Zhu [17].

The present paper describes an experimental research dedicated to characterization of a stratified honeycomb core material in the case of low energy impact. The behavior of specimens made of paper honeycomb core with different height and composite skins with two or three layers was assessed in order to find the one with the best behavior from the point of view of impact energy absorption. Experimental results were validated using a finite element simulation of a low velocity impact in the same conditions as those used in the experimental work.

2. SPECIMENS

The specimens were manufactured with a core made of resin impregnated paper (Fig. 2). For the skins, polymeric resin reinforced with glass fiber was casted on a plane surface in layers of 1 mm thickness. Before the plates became dry, the honeycomb stratified material was realized using polymeric resin as adhesive between the core and skins.

All specimens were cut from the obtained stratified material with the dimensions 60 × 60 mm as seen in Fig. 3a. Thus, a total of seven full cells exist in each specimen. The specimens were cut in such a way as to obtain double symmetry.

Four types of specimens were considered for the dynamic analyses, denoted as: **Specimen A** – core height of 22 mm and skin made of two layered composite plate, **Specimen B** – core height of 22 mm and

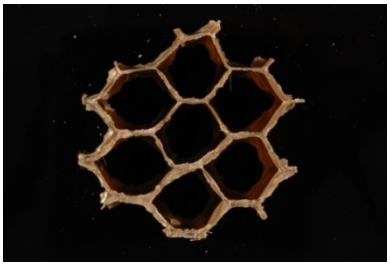

Fig. 2 – The core.

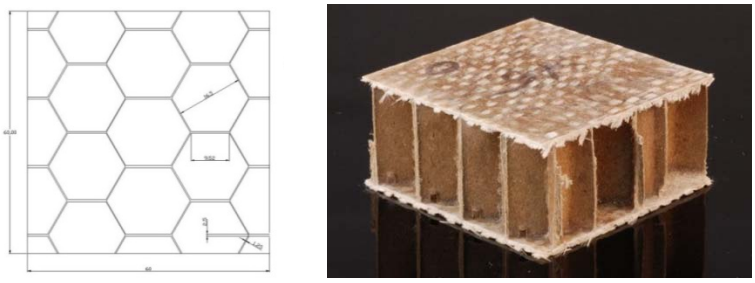

a b

Fig. 3 – a) Configuration of honeycomb cells in the specimen;
b) view of specimen C.

skin made of three layered composite plate, **Specimen C** – core height of 26 mm and skin made of two layered composite plate, and **Specimen D** – core height of 26 mm and skin made of three layered composite plate. Five specimens of each type were tested and results were averaged. In Table 1, the characteristics of the considered specimens are listed. Fig. 3b presents a view of specimen C [18].

Table1

Description of the specimens

Specimen type	Nr. of tested specimens	Core height	Dimensions of the skin [mm]	Nr. of layers for skin	Thickness of a skin layer [mm]
A	5	22	60 × 60	2	1
B	5	22	60 × 60	3	1
C	5	26	60 × 60	2	1
D	5	26	60 × 60	3	1

In order to obtain the elastic constants of the materials, tensile tests were undertaken using an INSTRON universal testing machine for eight plane specimens manufactured from the material of the composite skin and cut on the direction of the fibers. For the core, compression tests were performed [18]. The average values of the elastic constants of the materials are presented in Table 2.

It should be mentioned that Young's modulus of the skin material on the direction perpendicular to the fibers is about 10 % lower than the one on the fibers direction while for Poison's ratio the difference is not significant. The mass density of the composite face was measured and a value of 2 440 kg/m^3 was obtained, while the mass density of the bulk material of the core was taken as 350 kg/m^3 [19].

Table 2

Mechanical characteristics of the materials on the direction of fibers

	Impregnated paper	Composite skin
Young's modulus [MPa]	1 200	90 120
Poisson's ratio ν	0.35	0.33

3. EXPERIMENTAL MEASUREMENTS AND RESULTS

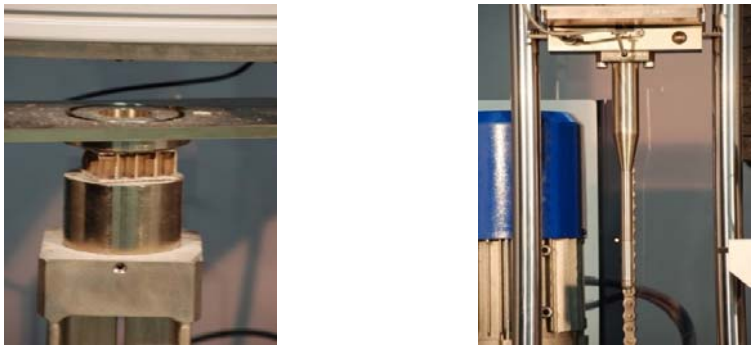

a b

Fig. 4 – a) – The gripping system; b) the impactor.

The specimens were subject to a drop-test using the Instron CEAST 9340 floor standing impact system, which provides impact energy between 0.3 … 405 J. The impact hammer, equipped with a force cell, had a weight that can be chosen between 2 and 30 kg. The control of the impact was done using a hammer with a weight of 4.9 kg and three different impact velocities: 1.43 m/s, 1.75 m/s and 2.02 m/s in order to obtain three values of the impact energy: 5 J, 7.5 J and 10 J, for each of the four considered types of specimens. The specimens were fixed in the testing machine by placing beneath each specimen a hollow support cylinder with an external diameter $D = 60$ mm and an internal diameter $d = 40$ mm. Above the specimen, a fastener acted by two hydraulic cylinders was placed, fixing the specimen through a ring having the same diameters as the support cylinder (Fig. 4a). The impactor (Fig. 4b) is coaxial with the fixation ring and the support cylinder. Thus, an impact in the center of the specimen is ensured. The variations of the impact force and strain energy, parameters that can evaluate the effects of impact, were obtained using the data acquisition system of the equipment. For each impact energy and each specimen, five tests were performed and the results were averaged. Figure 5 presents one of the specimens C, impacted with different energy values. Figures 5a, b and c show the effect of an impact with energy of 5 J. In Fig. 5a, the face opposite to the impacted one is shown. Figure 5b presents the impacted area while in Fig. 5c a side view is shown, where a light deformation of the core is visible. The same sequence of three figures is presented for the energy of 7.5 J (Fig. 5d, e and f) and for the energy of 10 J (Figs. 5g, h and i). For both cases, the skin is cracked but without penetration. The side views show damage of the core, which is more severe for the 10 J case.

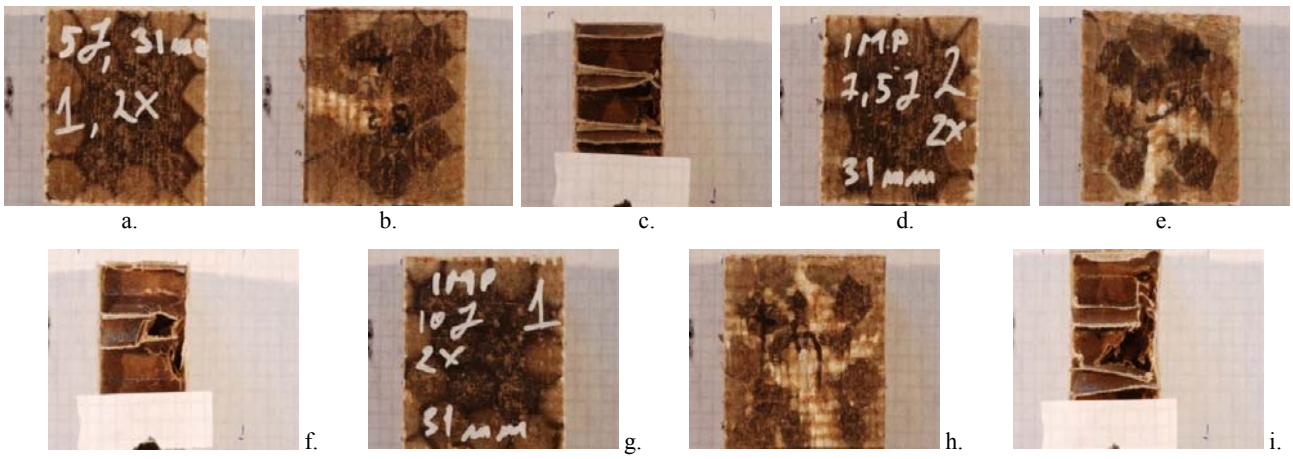

a. b. c. d. e.

f. g. h. i.

Fig. 5 – Specimen C after impact: a, b and c – impact with an energy of 5 J;
d, e and f – impact with an energy of 7.5 J; g, h and i – impact with an energy of 10 J.

Studying the effect of impact for the other three types of specimen, one can notice that the deformation of the core is smaller than for specimen C. As an illustration, the impact behavior of specimen D is presented in the same three-picture sequence in Fig. 6, for the 10 J impact. One can see in Fig. 6b the cracks that are visible due to the penetration of the hammer. Also, in Fig. 6c it can be noticed that the honeycomb structure suffered very little damage due to impact. Similar conclusions can be drawn for specimens A and B, excepting the fact that penetration of the skin did not occur for specimen B. Thus, it can be underlined that specimens A, B and D have a more rigid behavior at impact while specimen C has a more elastic behavior. It deforms more and absorbs the impact waves better than the other three. That is why such structure may be used as protection at impacts since it fails by absorbing the impact waves which would not be transmitted to the protected object.

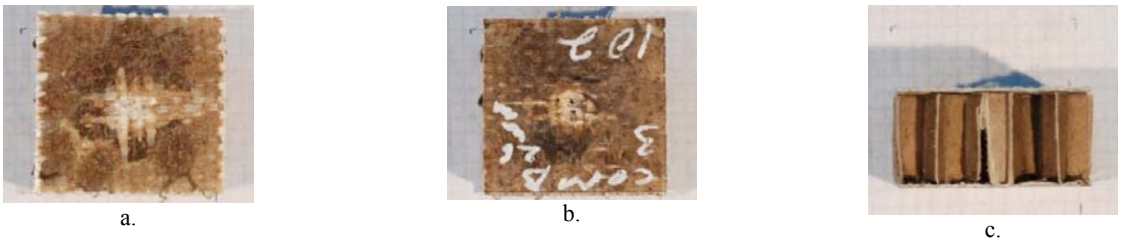

a. b. c.

Fig. 6 – Specimen D after impact with an energy of 10 J.

The variation of the impact force as a function of the tup displacement is shown in Figs. 7, 8, 9 and 10 for all four types of specimen. In the case of the 10 J impact, which is supposed to produce the greatest damages, a comparative graph of the variation of the impact force versus time is shown in Fig. 10 for all specimens.

The analysis of the graphs above reveals some interesting facts about the variation of the impact force. In the case of specimen A (Fig. 7), a maximum force of about 1 100 N can be noticed for the lower values of the impact energy, while in the case of the energy of 10 J, the maximum force is smaller (about 900 N). This can be explained by the fact that, in this last case, the hammer penetrated the skin. An impact force between 1 400 and 1 500 N was noticed for the case of specimen B (Fig. 8). In this case, no penetration was noticed regardless of the values of the impact force. For specimen C (Fig. 9) the maximum impact force was about 1 100 N for the energy of 5 J. Finally, the impact tests on specimen D (Fig. 10) showed forces between 1 200 N and 1 350 N. We can state that higher impact energy does not actually mean a higher impact force, since not all specimens were penetrated by the hammer.

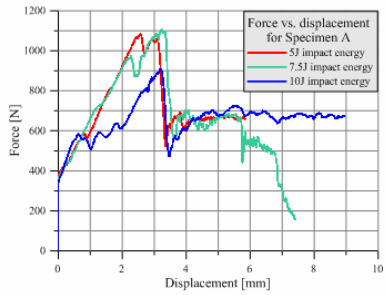

Fig. 7 – Variation of impact force with displacement for specimen A.

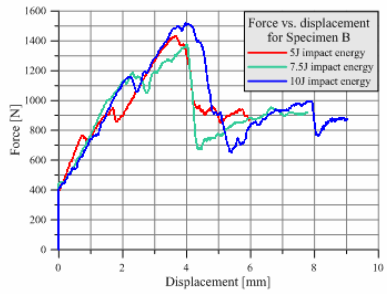

Fig. 8 – Variation of impact force with displacement for specimen B.

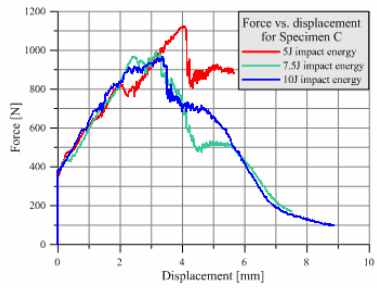

Fig. 9 – Variation of impact force with displacement for specimen C.

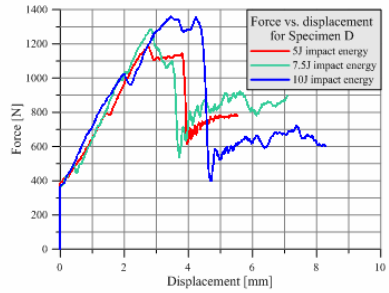

Fig. 10 – Variation of impact force with displacement for specimen D.

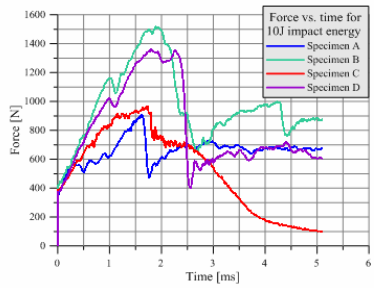

Fig. 11 – Variation of the impact force in time for all specimens in the case of an impact energy of 10 J.

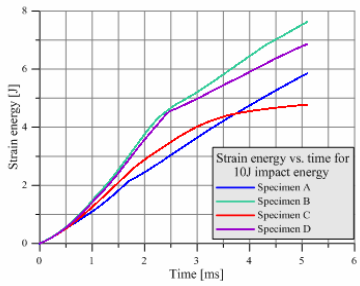

Fig. 12 – Comparative variation of strain energy in time for an impact energy of 10 J.

Analysis of the force variation with impact time from Fig. 11 reveals that specimens A, B and D have a similar behavior: after an increase of the force, it has a sudden drop (at about 1.5 … 1.7 ms for specimen A, 2.0 … 2.3 ms for specimen B and 2.4…2.5 ms for specimen D). Specimen C has a different behavior showing a slow decrease of the force after a very small drop at about 1.8 ms. The same specimen C shows also an important failure of the skin in the case of 10 J impact energy which explains the lower impact force obtained in this case. The results confirm the conclusions obtained from the visual inspection of specimens after impact, presented above.

The comparative variation of the strain energy in time in the case of the 10 J impact energy is shown in Fig. 12 for all specimens. The values of the strain energy can be used to calculate the average impact force, a parameter that may be taken into account when comparing the specimens from the point of view of impact behavior. This quantity is defined as the total absorbed strain energy (Fig. 12) divided by the maximum tup displacement (from Fig. 7 to Fig. 10). A comparison between the four considered specimens taking into account different parameters that can quantify the energy absorption and behavior at impact is presented in Table 3. Analysis of the comparative results from Table 3 can yield some conclusions about the best specimen configuration in terms of impact energy absorption. First, a more elastic behavior means a higher protection at impact: the specimen fails and deforms more absorbing thus the impact waves. That is why such structures may be used to cover objects that should get impact protection: these objects are protected since impact

waves would not be transmitted to the protected object or only a small part will be transmitted to the protected object. Also, if penetration of the skin does not appear, the protection to shock is better. Another conclusion regarding the behavior at impact is coming from the analysis of the force variation in time. If the drop of the force following the impact is slow then decelerations are lower and the amortization of the impact in time is better. Finally, a lower average impact force proves also a better behavior from the point of view of impact energy absorption.

Taking into account all the criteria presented in Table 3, one can conclude that specimen C is the best in terms of impact energy absorption.

Table 3

Comparison between the considered specimens regarding the behavior at impact

Specimen	**Damage of the core/type of behavior**	**Penetration of skin**	**Drop of impact force/ approximate time of drop [ms]**	**Average impact force [N]**
A	Small/rigid	Yes	Sudden/1.6	643
B	Small/rigid	No	Sudden/2.1	699
C	Big/elastic	No	Slow/1.8	543
D	Small/rigid	Yes	Sudden/2.4	840
Best behavior	***C***	***B, C***	***C***	***C***

4. NUMERICAL ANALYSIS

A numerical analysis was made in order to fully understand the impact process and to verify the correctness of the experimental results. For this, a 3D model of the specimen with the best behavior at impact – specimen C – was created and analyzed using the finite element method.

The numerical model respects the conditions of the experiment both in terms of boundary condition and of dynamic load. An impact hammer with the mass of 4.9 kg was modeled and set to strike the specimen in the center of the middle honeycomb cell with a speed of 2.02 m/s, the resulting impact energy being 10 J. A full model of the structure was considered. The model was meshed using three dimensional elements: 10 nodded tetrahedral elements were used to model the skins and the impact hammer, and 20 nodded brick elements were used to model the core. The minimum edge length of an element was set to 0.057 mm.

Several parameters were selected considering the results from the experimental tests and rules taken from [20]. A 5 ms time interval (the total time of impact obtained from the experimental data) was set for the program to complete the numerical calculus and also a 10^{-7} s minimum time increment was set. The choice of these parameters influences the running time and they should be chosen with small values but not as small as to influence the validity of results [21, 22]. Fig. 13 presents the numerical model, obtained and analyzed using the finite element software ANSYS [23]. A linear elastic behavior of the used materials was considered and the elastic constants were those from Table 2. In the case of the impact hammer, the material was steel with a Young's modulus of 200 GPa and Poisson's ratio of 0.3. The contour map of the equivalent von Mises stress is presented in Fig. 14.

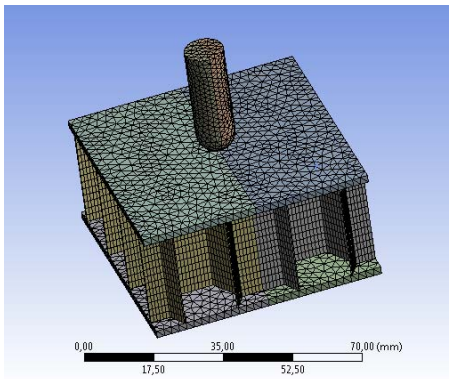

Fig. 13. – The numerical model
(17 218 nodes and 19 666 elements).

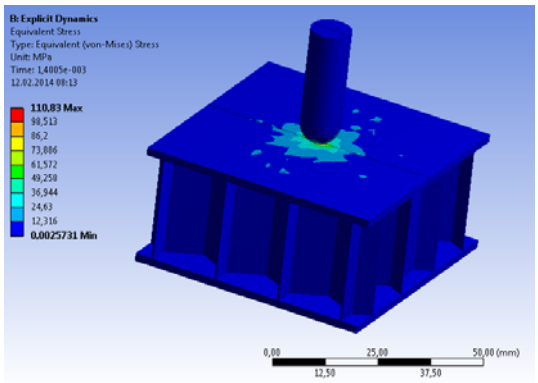

Fig. 14 – Contour map of the von Mises equivalent stress at t = 1.4ms.

The impact force was obtained as the product between the normal stress in the tup and the cross section area of the tup. A comparative graph between the numerical and experimental variation of the impact force in the studied case (specimen C, impact energy of 10 J) is plotted in Fig. 15. Only the graph in the linear elastic range of the stresses was presented since a linear elastic model was used. The graphs have a similar trend, with the numerical values slightly lower than the experimental ones. In order to evaluate the difference between the numerical and experimental results, the force values obtained numerically (plotted with a blue cross in Fig. 15 and obtained at an interval of approximately 0.19 ms) were fitted using a polynomial fit. Several polynomials were used and the closest to the numerical values was the one with a function of the fourth degree, in the form:

$$F = 350.497 + 394.662 \times t + 587.797 \times t^2 - 740.255 \times t^3 + 214.515 \times t^4.$$

Using this function, the difference between the numerical and experimental data was calculated for each value of the force at an interval of 0.01 ms and plotted in Fig. 16. One can see that the difference varies between – 4% and 9%. More precisely, the maximum difference is at t = 0.001 s and at t = 1.147 ms and has a value of 8.93%. Consequently, it can be stated that the agreement between the experimental and numerical values is good, validating thus the experimental analyses.

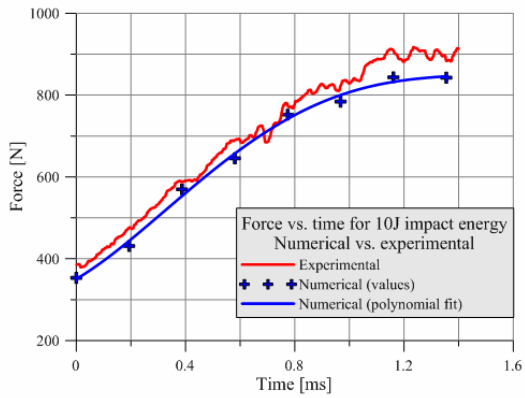

Fig. 15 – Comparison between the numerical and experimental variation of the impact force for a 10 J impact energy.

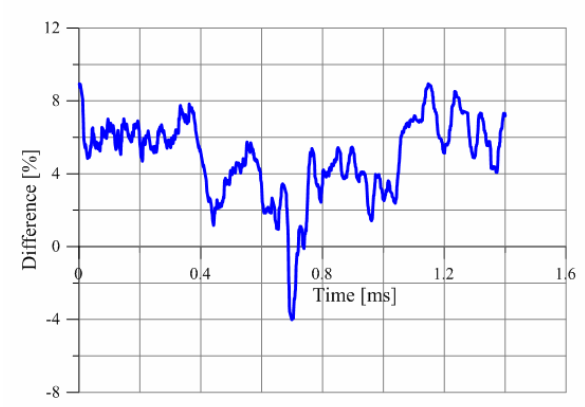

Fig. 16 – Difference between the experimental and numerical results for a 10 J impact energy.

4. CONCLUSIONS

The paper presents a model of calculus for low energy impact on a stratified honeycomb core material. The behavior of four types of sandwich specimens with honeycomb core made of resin impregnated paper and skins manufactured from polymeric resin reinforced with glass fiber was experimentally assessed through drop-tests with different values of the impact speed for the same mass of the impact hammer. The variation of the impact force and strain energy were monitored in order to find the specimen with the best behavior from the point of view of impact behavior. From the considered configurations, the one with a core of 26 mm height and two layered skin (specimen C) was chosen as the best. For this specimen, the variation of the force had a different trend compared to the other types of specimen: after an increase of the force, the decrease is slow showing lower decelerations and a better amortization of the impact. Meanwhile, for the other three specimens, the decrease of the force is very quick and steep. Also, specimen C exhibits a more elastic behavior which means a higher protection at impact: the specimen failed and deformed more absorbing thus the impact waves while the objects that are covered by a structure similar to the one of this specimen would be protected since waves would not be transmitted to the protected object. Both specimen C and specimen B did not present skin penetration, which means protection to impact is better. Finally, from the point of view of the average impact force, another parameter used to assess the impact behavior, specimen C presented the lowest value, which proves also a better behavior to impact.

Numerical simulations were undertaken for specimen C in the case of an impact energy of 10 J. Impact in the center of the specimen (which means center of the middle cell) was considered, in order to be similar with the experimental determinations. The same impact speed and mass of impact hammer were modeled in the finite element analysis. The numerical variation of the impact force versus tup displacement was extracted from the results and compared with the experimental one. A good agreement was noticed between the two sets of results showing thus the reliability of the experimental measurements.

The presented experimental research shows a methodology that can be successfully used in order to choose the best configuration honeycomb core – composite skin for practical industrial applications where protection to impact is important.

REFERENCES

1. *** http://www.netcomposites.com/guide/honeycomb-cores/46
2. A. WILBERT, W.Y. JANG, S. KYRIAKIDES, J.F. FLOCCARI, *Buckling and progressive crushing of laterally loaded honeycomb*, International Journal of Solids and Structures, **48**, pp. 803–816, 2011.
3. Y. AMINANDA, B. CASTANIÉ, J.J. BARRAU, P. THEVENET, *Experimental Analysis and Modeling of the Crushing of Honeycomb Cores*, Applied Composite Materials, **12**, pp. 213–227, 2005.
4. M. MEO, R. VIGNJEVICA, G. MARENGOB, *The response of honeycomb sandwich panels under low-velocity impact loading*, International Journal of Mechanical Sciences, **47**, pp. 1301–1325, 2005.
5. M. YAMASHITA, M. GOTOH, *Impact behavior of honeycomb structures with various cell specifications - numerical simulation and experiment*, International Journal of Impact Engineering, **32**, pp. 618–630, 2005.
6. A. CHAWLA, S. MUKHERJEE, D. KUMAR, T. NAKATANI, M. UENO, *Prediction Of Crushing Behaviour Of Honeycomb Structures*, International Journal of Crashworthiness, **8**, *3*, pp. 229–235, 2003.
7. P. GRIŠKEVIČIUS, D. ZELENIAKIENĖ, V. LEIŠIS, M. OSTROWSKI, *Experimental and Numerical Study of Impact Energy Absorption of Safety Important Honeycomb Core Sandwich Structures*, Materials Science (Medžiagotyra), **16**, *2*, pp. 119–123, 2010.
8. D. WANG. *Impact behavior and energy absorption of paper honeycomb sandwich panels*, International Journal of Impact Engineering, **36**, pp. 110–114, 2009.
9. C.C. FOO, L.K. SEAH, G.B. CHAI, *Low-velocity impact failure of aluminium honeycomb sandwich panels*, Composite Structures, **85**, pp. 20–28, 2009.
10. J.P.DEAR, H. LEE, S.A. BROWN, *Impact damage processes in composite sheet and sandwich honeycomb materials*, International Journal of Impact Engineering, **32**, pp. 130–154, 2005.
11. A.R. OTHMAN, D.C. BARTON, *Failure initiation and propagation characteristics of honeycomb sandwich composites*, Composite Structures, **85**, pp. 126–138, 2008.
12. A.N. PALAZOTTO, E.J. HERUP, L.N.B. GUMMADI, *Finite element analysis of low-velocity impact on composite sandwich plates*, Composite Structures, **49**, *2*, pp. 209–227, 2000.
13. T. BESANT, G.A.O. DAVIES, D. HITCHINGS, *Finite element modelling of low velocity impact of composite sandwich panels*, Composites Part A: Applied Science and Manufacturing, **32**, *9*, pp. 1189–1196, 2001.
14. M.Q. NGUYEN, S.S. JACOMBS, R.S. THOMSON, D. HACHENBERG, M.L. SCOTT, *Simulation of impact on sandwich structures*, Composite Structures, **67**, *2*, pp. 217–227, 2005.
15. M.D. AKIL HAZIZAN, W.J. CANTWELL, *The low velocity impact response of an aluminium honeycomb sandwich structure*, Composites Part B: Engineering, **34**, *8*, pp. 679–687, 2003.
16. K.W. KANG, H.S. KIMB, M.S. KIM, J.K. KIM, *Strength reduction behavior of honeycomb sandwich structure subjected to low-velocity impact*, Materials Science and Engineering: A, **483–484**, pp. 333–335, 2008.
17. G.B. CHAI, S. ZHU, *A review of low-velocity impact on sandwich structures*, Proceedings of The Institution of Mechanical Engineers Part L-Journal Of Materials-Design And Applications, **225**, *L4*, pp. 207–230, 2011.
18. H.A. PETRESCU, *Contributions to the Study of Behavior of Honeycomb Core Stratified Plates, Subjected to Static and Dynamic Loads*, (in Romanian), PhD Thesis, University Politehnica of Bucharest, 2011.
19. *** http://matweb.com/
20. M.A. CRISFIELD, *Non-linear Finite Element Analysis of Solids and Structures. I: Essentials*, J. Wiley and Sons, Chichester, West Sussex, England, 1997.
21. B.M. LUCCIONI, V.C. ROUGIER, *A plastic damage approach for confined concrete*, Computers and Structures, **83**, pp. 2238–2256, 2005.
22. Y. BENEVISTE, J. ABOUDI, *A Continuum Model for Fiber Reinforced Materials with Debonding*, International Journal of Solids and Structures, **20**, pp. 935–951, 1984.
23. *** ANSYS 15.0 – release notes, http://148.204.81.206/Ansys/150/ANSYS,%20Inc.%20Release%20Notes.pdf, ANSYSInc, Canonsburg, PA, 2013.

Received July 29, 2014